Biophysical Journal, Volume *111*

Supplemental Information

Mode of Action of a Designed Antimicrobial Peptide: High Potency against *Cryptococcus neoformans*

Aritreyee Datta, Vikas Yadav, Anirban Ghosh, Jaesun Choi, Dipita Bhattacharyya, Rajiv K. Kar, Humaira Ilyas, Arkajyoti Dutta, Eunseol An, Jayanta Mukhopadhyay, Dongkuk Lee, Kaustuv Sanyal, Ayyalusamy Ramamoorthy, and Anirban Bhunia

Mode of Action of A Designed Antimicrobial Peptide: High Efficiency in Killing the Human Fungal Pathogen *Cryptococcus neoformans*

Aritreyee Datta,[a,ψ] Vikas Yadav,[b,ψ] Anirban Ghosh,[a] Jaesun Choi,[c] Dipita Bhattacharyya,[a] Rajiv K. Kar,[a] Humaira Ilyas,[a] Arkajyoti Dutta,[d] Eunseol An,[c] Jayanta Mukhopadhyay,[d] Dongkuk Lee,[c] Kaustuv Sanyal,[b] Ayyalusamy Ramamoorthy,[e] and Anirban Bhunia*[a]

[a]Department of Biophysics, P-1/12 CIT Scheme VII (M), Kolkata 700054, India. [b]Molecular Biology and Genetics Unit, Jawaharlal Nehru Centre for Advanced Scientific Research, Bangalore 560064, India. [c]Department of Fine chemistry, Seoul National University of Science and Technology, Seoul 01811, Korea. [d]Department of Chemistry, Bose Institute, 93/1 APC Road, Kolkata 700009, India. [e]Biophysics and Department of Chemistry, University of Michigan, 930 University N Avenue, Ann Arbor, Michigan 48109-1055, USA.

ψBoth authors contributed equally to this work.

*To whom correspondence should be addressed: Dr. Anirban Bhunia, Department of Biophysics, P-1/12 CIT Scheme VII (M), Kolkata 700054, India, Telephone: (091) 33-2569-3336, Email: anirbanbhunia@gmail.com or bhunia@jcbose.ac.in)

Reagents:

Polymyxin B, Calcein, 1-N-phenyl napthylamine (NPN), cholesterol and ergosterol were purchased from Sigma Aldrich Co. (St. Louis, USA). POPC (1-palmitoyl-2-oleoyl-*sn*-glycero-3-phosphocholine), POPG (1-palmitoyl-2-oleoyl-*sn*-glycero-3-phospho-(1'-rac-glycerol) sodium salt), POPE (1-palmitoyl-2-oleoyl-*sn*-glycero-3phospho-ethanolamine) were purchased from Avanti Polar Lipids Inc. (Alabaster, AL) and used without further purification. 4, 4-dimethyl-4-silapentane-1-sulfonic acid (DSS), and deuterium oxide (D_2O) were purchased from Cambridge Isotope Laboratories, Inc. (Tewksbury, USA). Stock solutions of phospholipids and sterols were prepared in $CHCl_3$.All media components were obtained from Himedia. All other reagents and chemicals were from Acros Organics unless mentioned.

Zeta potential Measurements:

Briefly, overnight grown log phase cultures of *C. neoformans* in YPD broth, were washed twice and resuspended in 10 mM phosphate buffer of pH 7.4. 1 ml cell suspension of 10^5 cells/ml was incubated with 10 µM peptide, corresponding to its MIC, for 90 min. The same microbial suspension without the peptide was used as the control set. Both sets of suspension were taken in disposable zeta cells and read at 25 °C. The zeta potential for each sample was calculated using the Zetasizer software.

Live-dead staining assay:

Briefly, the cells were harvested, re-suspended in water and then stained with propidium iodide (PI) and SYTO9 dyes for 45 min. After incubation, the cells were imaged for presence of SYTO 9 (green) and PI (red) using fluorescence microscope. The images were captured on an Olympus microscope (Model BX51) using an Olympus DP71 camera. The images were further processed using Image Pro-Plus software, Image J, and Adobe Photoshop.

Spheroplasting and peptide-FITC conjugate localization assay:

C. neoformans cells were grown overnight in YPD at 30 °C. Overnight grown cells were harvested next day, washed with water and then resuspended in 10 ml of spheroplasting buffer (1M Sorbitol, 0.1M Citrate buffer pH 5.8, 0.01M EDTA pH 8.0) to final concentration of 10^7 cells/ml. The cells were then treated with 20 mg of lysing enzyme (Sigma, cat no. L1412) for 2 h at 37 °C to get 40-50% spheroplasts. This mix of spheroplasted and normal cells was then incubated with 1 µM peptide-FITC conjugate for an h at 30 °C. These treated cells were observed under microscope to determine the localization of peptide in these spheroplasted cells.

Calculation of solution state NMR derived structures:

Depending upon the intensities of the NOE cross peaks in the NOESY spectra of the peptide in presence of *C. neoformans* cells, the NOE volume integrals were differentiated qualitatively into strong medium and weak peaks for NMR-derived structure calculations. This information was next converted to inter-proton upper bound distances of 3.0, 4.0 and 5.0 Å for strong, medium and weak, respectively, while the lower bound distance was fixed to 2.0 Å. The backbone dihedral angle (Φ) phi and psi (ψ) of the peptide was kept flexible (-30° to -120° and 120° to -120°, respectively) for all non-glycine residues to limit the conformational space. Hydrogen bonding constraints have been excluded in the structure calculations. All structure calculations were performed using the CYANA program *v2.1* (1) with iterative refinement of the structure based on distance violation. PyMol, software was used to analyse the NMR-derived ensemble structures. The stereochemistry of the structures was checked using Procheck.(2) The calculated structures were deposited to protein data bank (PDB) with accession codes of 2N9M.pdb (Conformation 1) and 2N9N.pdb (Conformation2) for VG16KRKP in *C. neoformans* cell suspension.

Docking and MD simulation studies:

A detailed description of the dynamic behavior for VG16KRKP bound to GG28 (duplex DNA) is as follows. In particular, the interaction is bound to occur between the negatively charged phosphate backbone and the positively charged residues such as Arg3, Lys6, Arg7, Lys8, and Lys14. The binding association between these amino-acids and nucleic acid backbone is found mainly in the minor groove region, which maintains a strong association throughout the MD simulation time scale, as depicted form the movie SV1. Interestingly, the peptide structure was found to maintain a partial helical structure at its C-ter region, turn structure at N-ter and central region. Interestingly, other residues that are intermediate from N-ter to central region (Ala2-Lys8) are found to have a secondary structural transition with respect to the starting confirmation of peptide in the MD simulation. Such structural transition can be accounted from α-helix to 3_{10} helix and towards beta-strand structure. The correlation of structural information obtained from MD simulation matches with the deconvolution data obtained from CD; the minute variations among the information sets, however, can be attributed to the adopted force field (theoretical study) and Brownian motion (experimental study). Overall, the binding association between VG16KRKP and duplex DNA is bound to be stabilized from the MD simulation that confirms a restriction of nucleobase movement in the binding region. The residues involved in the binding between VG16KRKP and duplex DNA are represented in stick conformation, which can be visualized in SV1 from the link.

The conformation for VG16KRKP in GG28 was also determined from the MD simulation that is correlated with RMSD values. As mentioned in the main text, the docked conformation display Hydrogen bonding between Arg3-dC17, Lys6-dC17, and Arg7-dC11. Though these hydrogen bondings are found consistent with the MD simulation time scale, there are other polar contacts, which emerge in the MD simulation time scale. The rationale for identifying these hydrogen bonding are that the ubiquitous nature of hydrogen bonding are essential for the governance of biological phenomena (3). Other hydrogen bondings such as Lys14-dC17, Val1-dC17, and Lys8-dA10 provide additional energy to the complex stability between VG16KRKP and GG28. Since each hydrogen bonding energy provides a stability of ~ 2 kcal/mol, total columbic energy estimated to be ~ 10 kcal/mol for the binding of peptide-DNA complex. The conformational analysis of the peptide in the presence of GG28 is also accounted from the time scale (Figure S2E). The side-chain of all the residues of VG16KRKP are shown in stick representation that reflects the dynamics of peptide. The position of N-ter and C-ter atoms can be found in the figure as blue and red spheres, respectively that accounts for its gyration radius.

Solid state NMR Sample Preparation:

For ^{31}P solid state NMR, 2 mg of POPC or 7:3 POPC/POPE, dissolved in $CHCl_3$, was used for each sample preparation and an appropriate amount of ERG (dissolved in $CHCl_3$) was mixed with the POPC/POPE sample. The mixed samples were dried under stream of nitrogen and then under vacuum-dry oven (30° C) overnight to completely remove any residual solvent. Tris buffer (10 mM Tris, pH 7.4) was added to samples to hydrate lipid film. The hydrated samples were vortexed for 2 min above the lipid phase transition temperature and freeze-thawed using liquid nitrogen at least 4 times to ensure a single lamellar vesicle. To obtain uniform size of large unilamellar vesicles (LUVs) of 1 μm in diameter, the LUVs were extruded through polycarbonate filters (pore size of 1 μm, (Nuclepore® Whatman, NJ, USA) mounted in a mini extruder (Avanti Polar Lipids, AL, USA) fitted with two 1.0 ml Hamilton gastight syringes (Hamilton, NV, USA). Samples were typically subjected to 23 passes through filter. An odd number of passages were performed to avoid contamination of the sample by vesicles that have not passed through the first filter. The VG16KRKP peptide solution, dissolved in Tris buffer, was added to LUVs to prepare the appropriate final peptide concentration:lipid molar ratio, making a final sample volume of 150μl.

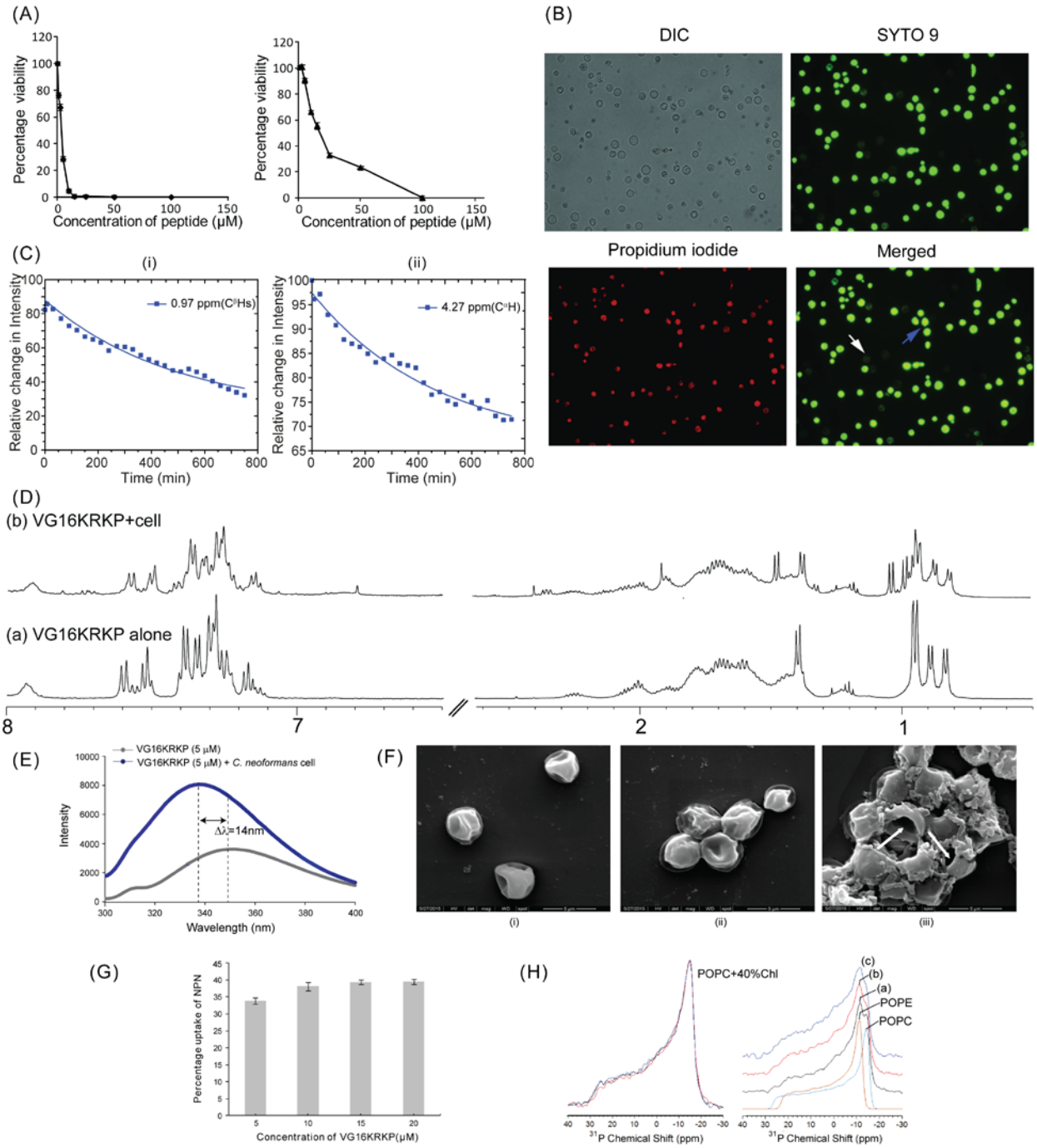

Figure S1. **Membrane perturbation of *C. neoformans* cells upon VG16KRKP binding**. (A) Dose response curve of VG16KRKP against 10^5 cells/ml (left panel) and 10^6 cells/ml of *C. neoformans* (right panel). (B) Fluorescence based live-dead staining to show the differentially stained cells after treatment with the peptide. The dead cells are stained with propidium iodide and are marked by blue arrow while live cells, stained with SYTO9 are marked using white arrow. (C) A time dependent plot of relative change in intensity in the proton resonances of the 1D NMR spectra of VG16KRKP upon addition of *C. neoformans* cells, showing a decrease in the resonance intensities of both the CαH and CβH protons of VG16KRKP. (D) Selected regions of the 1D proton NMR spectra showing broadening of peptide resonances upon addition of live *C. neoformans* indicating binding. (E) Fluorescence emission spectra of Trp present in VG16KRKP upon addition of live *C. neoformans* cells showing 14 nm blue shift indicating

peptide binding to cell surface. (F) SEM image of (i) *C. neoformans* cells treated with VG16KRKP after 15 min, (ii) 30 min and (iii) 90 min, showing gradual shrinkage and formation of crescent shaped bowl like structures that indicate osmolytic shock and membrane compromise. (G) Bar plot showing the percentage of NPN dye uptake by *C. neoformans* cells upon treatment with increasing concentrations of VG16KRKP. Approximately 40% of NPN dye uptake was observed upon treatment with 20 µM peptide, indicating the membrane perturbation of the cell by peptide treatment. The untreated control, however, showed 0% uptake and therefore is not shown in the graph. (H) ^{31}P powder spectra of POPC/40% cholesterol (left panel) and Simulated POPC (Blue) and POPE (orange) (right panel) (a) experimental ^{31}P powder spectra of 5:4:3 POPC/POPE/ERG LUVs (b) 2 mol% and (c) 4 mol% VG16KRKP addition into the LUVs.

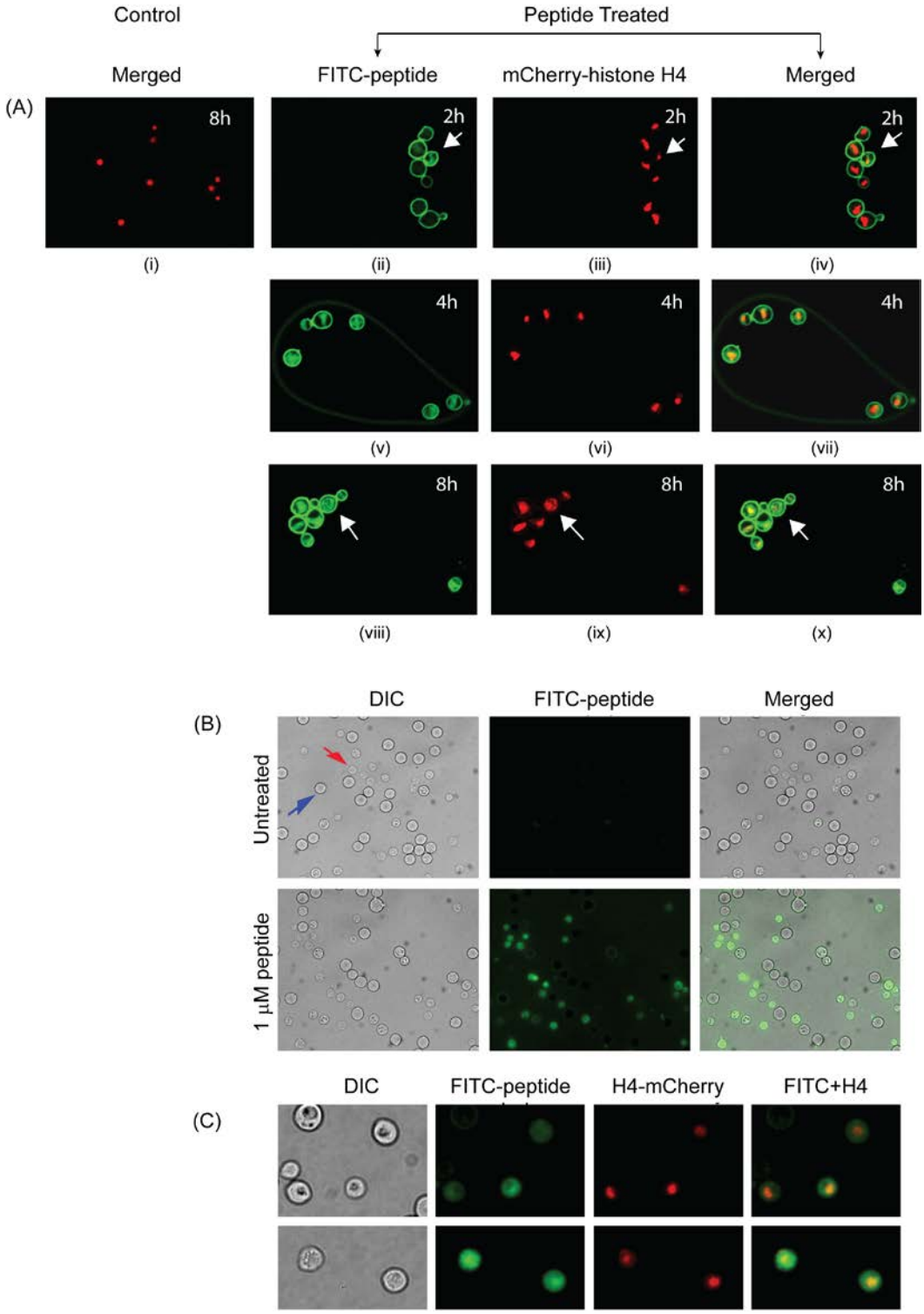

Figure S2. **Nuclear localization of VG16KRKP visualized by confocal microscopy. (**A) Confocal images of *C. neoformans* histone H4-mCherry cells incubated in absence of peptide for 8 h (i) or in the presence of FITC tagged VG16KRKP incubated for 2 h (ii, iii, iv) , 4 h (v, vi, vii) and 8 h (viii, ix, x) with ii, v, and viii showing the images through FITC channel, iii, vi and ix showing the images through mCherry channel and i, iv, vii and x showing the FITC/mCherry superimposed/merged images. ii, iii, and

iv show the FITC tagged VG16KRKP to be majorly membrane bound at the end of 2 h with some localization inside the cell marked with an arrow. v, vi and vii show the peptide to be located at the membrane and inside the cell, at the nucleus in some cells. viii, ix and x show the peptide to be membrane bound and localized in the nucleus with an observable enlargement of the nucleus in few cases as marked by the arrow depicting nuclear fragmentation. (B) Peptide-FITC was localized within the cells which were spheroplasted (marked by red arrow) whereas it was present on cell wall/membrane in non-spheroplasted cell (marked by blue arrow). Untreated cells did not show any localization (upper panel). (C) Peptide-FITC conjugate was localized in cells expressing H4-mCherry as marker for nucleus. As seen in the figure, peptide was marginally more enriched into the nuclear compartment compared to rest of the cell.

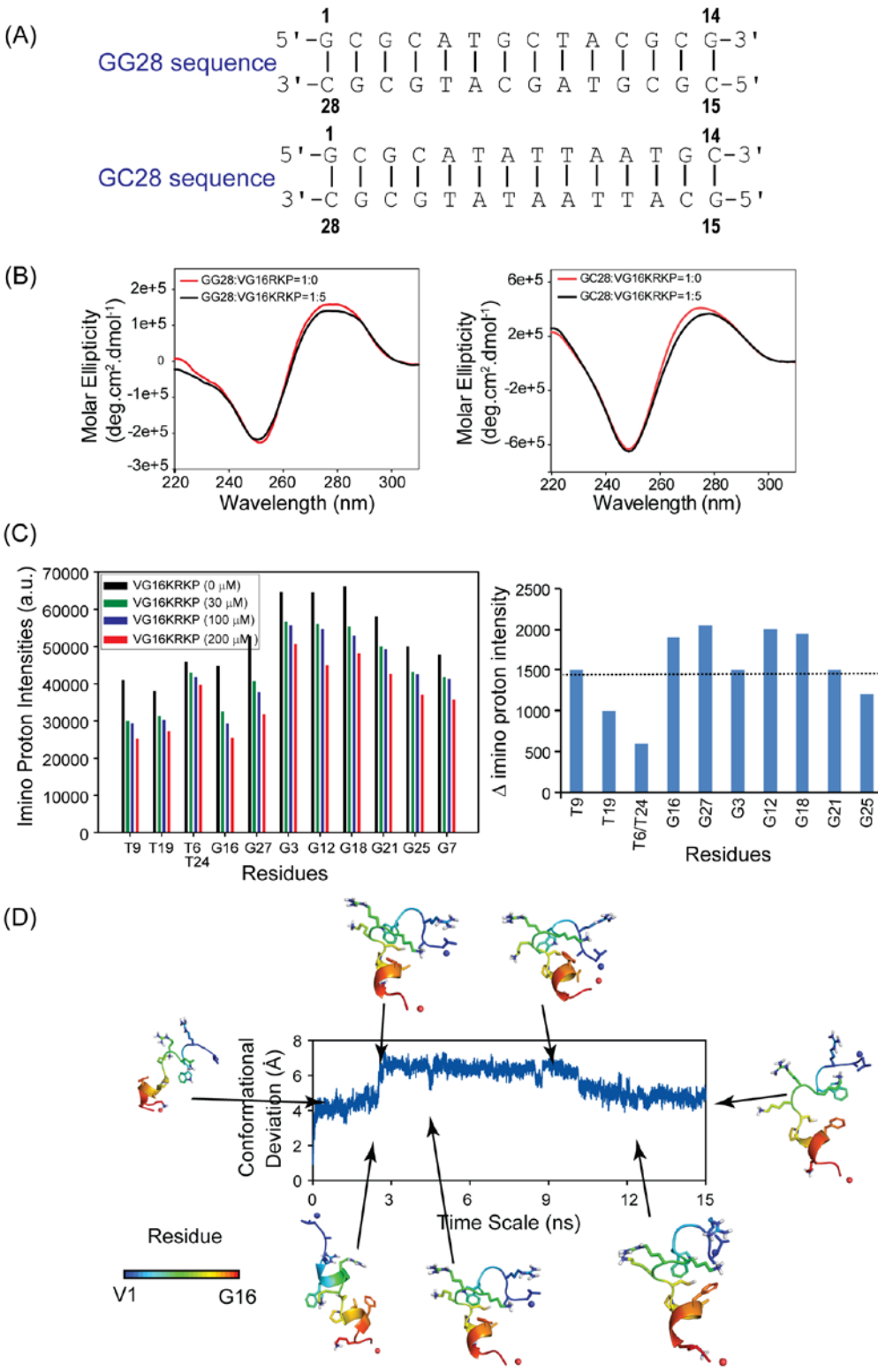

Figure S3. DNA binding abilities of VG16KRKP. (A) Scheme showing the sequence of the two DNA sequences, GG28 and GC28. (B) The CD signature of the DNA sequences GG28 and GC28 alone and upon addition of VG16KRKP at a molar ratio of 1:1. (C) Bar plot of imino proton resonances of the DNA sequence GG28 showing a steady decrease upon addition of increasing concentrations of peptide (left

panel). The quantitative decrease in imino proton intensity of GG28 in the presence of VG16KRKP (with a molar ratio of GG28 : VG16KRKRP=1:1) (right panel). The dotted line indicates the average decrease in intensity. (D) Structural snapshots of VG16KRKP bound to GG28, based on structural deviations with reference to time scale.

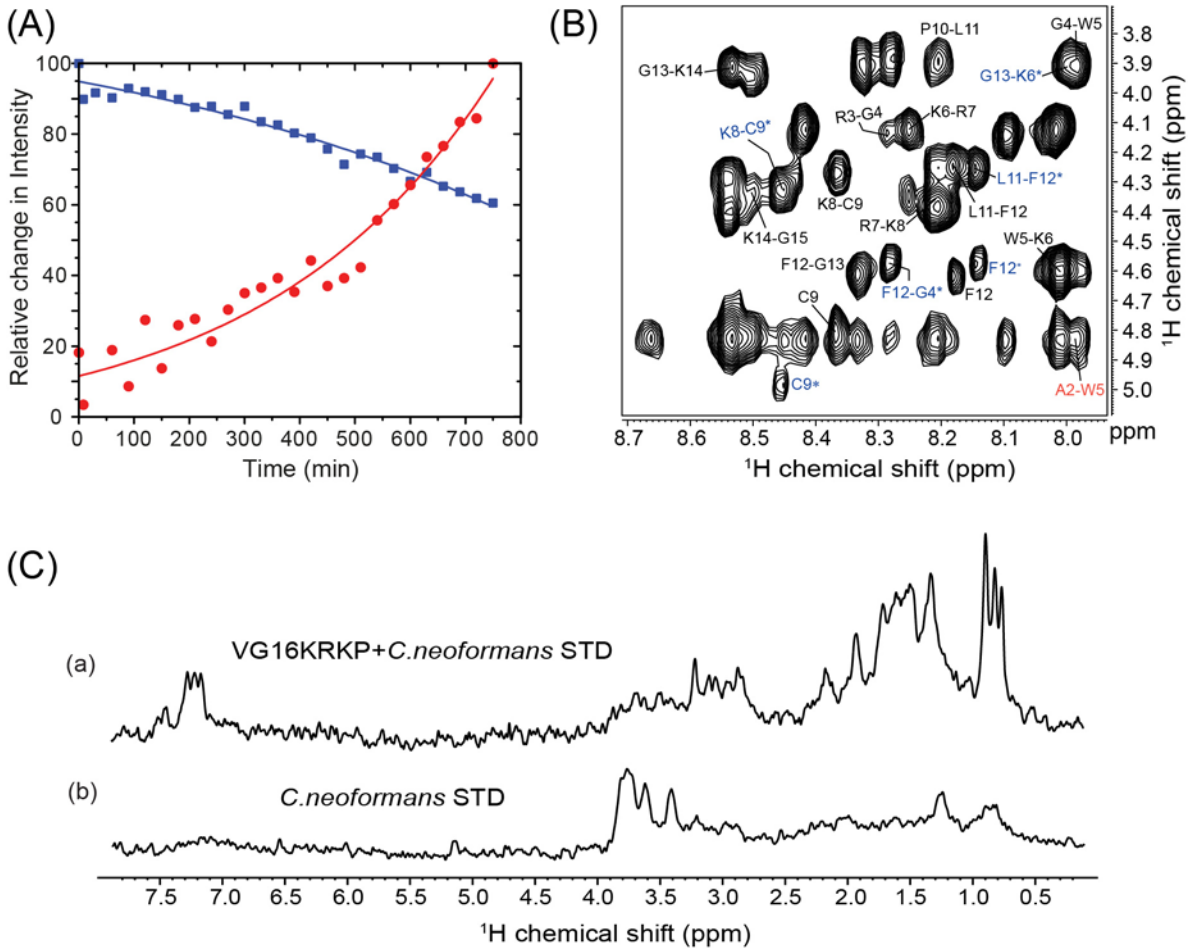

Figure S4. NMR structural parameters of the *C. neoformans* bound Conformations of VG16KRKP. (A) Plot showing reduction in the resonance intensities of the main peak of Trp aromatic $N^{\varepsilon}H$ proton in association with an increase in the resonance intensity of a sub peak corresponding to an emergence of a second conformation. (B) Fingerprint region of the tr-NOESY spectra of VG16KRKP in presence of *C. neoformans*, showing the presence of two conformations: Conformation 1 is marked with asterisk in blue, and Conformation 2 is marked in red; (C) Saturation transfer difference (STD) spectra of (a) VG16KRKP in presence of *C. neoformans* cells and (b) STD spectra of *C. neoformans* cells alone.

Supporting references

1. Güntert, P., Mumenthaler, C., and Wüthrich, K. (1997) Torsion angle dynamics for NMR structure calculation with the new program DYANA. *J. Mol. Biol.* **273**, 283-298

2. Laskowski, R. A., Rullmannn, J. A., MacArthur, M. W., Kaptein, R., and Thornton, J. M. (1996) AQUA and PROCHECK-NMR: programs for checking the quality of protein structures solved by NMR. *J. Biomol. NMR* **8**, 477-486
3. Katharina, W., Jens, T., Stefan, Z., and Barbara, K. (2010) Estimating the Hydrogen Bond Energy. *The Journal of Physical Chemistry* **114**, 9529-9536